Parallel Electric Fields Associated with Double Layers in Kappa Distributed Space Plasmas

Saba Khalid, Muhammad Nouman Sarwar Qureshi*, Umm e Hira and Shoaib Akhtar
Department of Physics, GC University, Lahore 54000, Pakistan
***Correspondence**: noumansarwar@gcu.edu.pk

Citation | Saba Khalid, Qureshi. M. N. S, Umm e Hira, Akhtar. S, "Parallel Electric Fields Associated with Double Layers in Kappa Distributed Space Plasmas", IJIST, Vol. 07 Issue. 01 pp 664-674, March 2025
Received | Feb 21, 2025 **Revised |** March 27, 2025 **Accepted |** March 29, 2025 **Published |** March 30, 2025.

Parallel electric field structures associated with double layers (DLs) provide the best explanation for the physical mechanism underlying charged particle energization acceleration at sites of magnetic reconnection. In-situ measurements of reconnection sites by various satellites such as MMS, THEMIS, and FAST confirmed the connection of charged particle energization with the large parallel electric fields in the auroral regions, Earth's plasma sheet, and the separatrix region of the magnetosphere. We employed the fully nonlinear Sagdeev potential technique and multi-fluid theory for electron-ion plasma to find double-layer solutions and the accompanying electric field at the reported sites. Considering electrons to be kappa distributed, we have taken into account the ion inertial effect. Specifically, at non-Maxwellian effective temperature scales, parallel electric fields related to the Alfvénic double layer have been studied and compared with the observations. We have shown that the nonthermal parameter kappa and Alfvénic Mach number M_A considerably alter the properties of DLs and the associated electric field of kinetic Alfvén waves.

Keywords: Double layers; Kappa distribution; Electric field structures; Kinetic Alfven waves

Introduction:

Magnetic reconnection is widely studied in both space and laboratory plasmas for its role in converting magnetic energy into plasma energy through heating and particle acceleration. The potential mechanisms behind the acceleration of charged particles in space plasmas were reported in many studies [1][2][3][4]. Nonetheless, field-aligned double layers provide a more credible explanation for particle acceleration in space plasmas [2][5][6][7]. In both natural and artificial plasma environments, double layers, non-linear structures with parallel potential structures and related electric fields are a source of charge particle energization. Charged particles can be energized by these field-aligned electric fields up to energies of about 10 KeV [8].

Kinetic Alfven waves are ubiquitous in space and astrophysical plasmas and enable energy transfer between electromagnetic fields and plasma particles through Landau damping and transit-time interactions, making KAWs essential for particle acceleration, plasma heating, and anomalous transport in both space and laboratory plasmas [9].

Observations from satellites such as Freja, FAST, and MMS have confirmed the interaction of KAWs with plasma particles, leading to energy exchange. These waves also interact with MHD-scale Alfvén waves, ion cyclotron waves, lower hybrid waves, and Langmuir waves. Additionally, studies have explored the effects of adiabatically trapped electrons on coupled kinetic Alfvén-acoustic (CKAA) waves in low-β and degenerate plasmas [10][11].

We were prompted to investigate double layers associated with Alfven waves in the various regions of space plasmas because of the significant attention that double layers and parallel electric fields have received in recent decades. Several space observations revealed that the particle distribution profile contained high energy tails as compared to Maxwellian tails. Such superthermal tails in the electron distribution function profile are often explained and fitted with an inverse power law distribution function in velocity space. First observations of these high-energy tails were reported in the plasma sheet and explained using the Kappa distribution function, which is also known as the generalized Lorentzian distribution [12]. The spectral index ϰ is a measure of the concentration of high-energy particles creating the tail of the distribution profile. This non-thermal distribution profile reduces to thermal as $\kappa \rightarrow \infty$. In this paper, we have examined the parallel electric fields and double layers in superthermal plasmas at effective temperature scales.

Objectives:

The objectives of this study are to investigate double-layer potential structures associated with Alfven waves in the plasma regions where electrons are considered to be following the non-Maxwellian distribution function. Also, we want to analyze our results in light of the real value plasma parameters observed by THEMIS in the space plasma regions where double-layer structures have been observed.

Methodology:

Basic Equations:

We consider a collisionless, magnetized electron-ion plasma in which electrons are considered as kappa distributed. For such a plasma, we will consider plasma fluid and employ two potential theories which valid for a low beta plasma, i.e. $\frac{m_e}{m_i} \ll \beta' \ll 1$. The ambient magnetic field $B_z = B_o, B_x = 0,$ and by employing the two potential theories [13], where the geometry of the wave lies in the x-z plane, such as

$$E_{\parallel} = -\frac{\partial \psi}{\partial z},\ E_{\perp} = -\frac{\partial \phi}{\partial x},\ \ E_y = 0 \qquad (1)$$

Considering the geometry of the system, the fluid set of equations for such plasma having a current density $j_z = n_e e(v_{iz} - v_{ez})$ is

$$\frac{\partial n_i}{\partial t} + \frac{\partial}{\partial x}(n_i \boldsymbol{v}_{ix}) + \frac{\partial}{\partial z}(n_i \boldsymbol{v}_{iz}) = 0 \tag{2}$$

$$\frac{\partial v_{ix}}{\partial t} + v_{ix}\frac{\partial v_{ix}}{\partial x} + v_{iz}\frac{\partial v_{ix}}{\partial z} = -\frac{e}{m_i}\frac{\partial \phi}{\partial x} + \Omega_i v_{iy} \tag{3}$$

$$\frac{\partial v_{iy}}{\partial t} + v_{ix}\frac{\partial v_{iy}}{\partial x} + v_{iz}\frac{\partial v_{iy}}{\partial z} = -\Omega_i v_{ix} \tag{4}$$

$$\frac{\partial v_{iz}}{\partial t} + v_{ix}\frac{\partial v_{iz}}{\partial x} + v_{iz}\frac{\partial v_{iz}}{\partial z} = -\frac{e}{m_i}\frac{\partial \psi}{\partial z} \tag{5}$$

$$\frac{\partial^4(\phi-\psi)}{\partial x^2 \partial z^2} = \mu_o e\left[\frac{\partial^2 n_e}{\partial t^2} + \frac{\partial^2(n_i v_{iz})}{\partial t \partial z}\right] \tag{6}$$

Here, ψ and ϕ are electrostatic potentials along the z and x directions respectively, $\Omega_i = \frac{e B_o}{m_i}$, is the ion-cyclotron frequency. β' Is plasma beta at a modified temperature scale? The relation for electron density is

$$n_e = n_{eo}[1 + \alpha_1 \Psi + \alpha_2 \Psi^2 + \alpha_3 \Psi^3] \tag{7}$$

The coefficients α_1 and α_2 for κ-distribution function are

$$\alpha_1 = \frac{\left(\kappa-\frac{1}{2}\right)}{\left(\kappa-\frac{3}{2}\right)} \tag{8}$$

$$\alpha_2 = \frac{\left(\kappa-\frac{1}{2}\right)\left(\kappa+\frac{1}{2}\right)}{2\left(\kappa-\frac{3}{2}\right)^2} \tag{9}$$

$$\alpha_3 = \frac{4(\kappa^2-1)(2\kappa+3)}{6(2\kappa-3)^3} \tag{10}$$

where $\Psi = \frac{e\,\psi}{T_\kappa}$ is normalized electrostatic potential and T_κ Is modified temperature for κ- distributed plasma.

The spectral index κ defines the nonthermal of the kappa distributed particles and measures the slope of the energy profile of high energy particles under the constraint that $\kappa > 3/2$. In the limiting case, when $\kappa \to \infty$, the kappa distribution function reduces to the Maxwellian distribution function.

Assuming that the equation of state in a nonthermal system is similar to that in an ideal gas, the pressure induced by nonthermal particles can be written as $p_\kappa = n_e T_\kappa$. Therefore, the induced pressure can be calculated as $p_\kappa = n_o m_e < v^2 >_\kappa$. Here $< v^2 >_\kappa = \int v^2 f_\kappa(v_e, \psi) dv$ is the mean-square velocity of the κ- distributed particle and the subscript f_κ Defines the kappa distribution function.

$$< v^2 >_\kappa = \frac{2\kappa}{2\kappa-3}\frac{k_B T}{m} \tag{11}$$

The standard expression of mean square velocity can be recovered from the above Eq. (11) $\kappa \to \infty$ and the ideal gas relation for κ-distributions can be written as

$$p_\kappa = \frac{1}{3}nm < v^2 >_\kappa = \frac{1}{3}nm\frac{2\kappa}{2\kappa-3}\frac{k_B T}{m} = nk_B T_\kappa \tag{12}$$

where T_κ Is the modified temperature for the corresponding distribution given as

$$T_\kappa = \frac{2\kappa}{2\kappa-3}T_e \tag{13}$$

The modified temperature T_κ Essentially represents the local thermal energy of non-Maxwellian electrons [14][15]. In the limiting case ϰ→∞ , T_q reduces to T_e [16], the thermal energy of Maxwellian distributed electrons. The non-Maxwellian modified temperatures T_κ Will be positive when $\kappa > 3/2$.

Linear Analysis:

Upon linearizing and solving Eqs. (2)-(6) and making use of Eq. (7), under the limit that $\omega^2 = V_A^2 {k_z}^2 \ll \Omega_i^2$, we obtain the following linear dispersion relation for coupled kinetic Alfven acoustic waves CKAA wave [10].

$$\left(1-\frac{V_A^2 {k_z}^2}{\omega^2}\right)\left(1-\frac{{c_s}^2{k_z}^2}{\alpha_1\omega^2}\right)=\frac{V_A^2{k_z}^2}{a\omega^2}\lambda_s \quad (14)$$

Here $V_A=\frac{B_o}{\mu_o n_i\, m_i}$ Is the Alfven velocity, $c_s=\sqrt{\frac{T_\kappa}{m_i}}$ Is the ion sound speed, $\rho_s=\frac{c_s}{m_i}$ and $\lambda_s=k_x^2\rho_s^2$. In the limiting case, as phase velocity becomes much larger than the sound velocity, the linear dispersion relation of CKAA waves reduces to the dispersion relation of KAWs, as given [17]

$$\omega^2={V_A}^2{k_z}^2\left(1+\frac{\lambda_s}{\alpha_1}\right)$$

Nonlinear Analysis for Double Layer Solution of CKAA Waves:

Fully nonlinear treatment of fluid set of equations (2)-(7) is done by employing Sagdeev potential approach. Normalizing our set of equations and introducing a co-moving frame as $\xi=K_xX+K_zZ-M\tau$, we get

$$-M\frac{\partial N_i}{\partial\xi}+K_x\frac{\partial}{\partial\xi}(N_iV_{ix})+K_z\frac{\partial}{\partial\xi}(N_iV_{iz})=0 \quad (12)$$

$$-M\frac{\partial V_{ix}}{\partial\xi}+(K_xV_{ix}+K_zV_{iz})\frac{\partial V_{ix}}{\partial\xi}=-K_x\frac{\partial\Phi}{\partial\xi}+\Omega_iV_{iy} \quad (15)$$

$$-M\frac{\partial V_{iy}}{\partial\xi}+(K_xV_{ix}+K_zV_{iz})\frac{\partial V_{iy}}{\partial\xi}=-\Omega_iV_{ix} \quad (16)$$

$$-M\frac{\partial V_{ix}}{\partial\xi}+(K_xV_{ix}+K_zV_{iz})\frac{\partial V_{iz}}{\partial\xi}=-K_z\frac{\partial\Psi}{\partial\xi} \quad (17)$$

$$\frac{K_x^2\beta'}{2}\frac{\partial^4}{\partial\xi^4}(\Phi-\Psi)=M^2\frac{\partial^2}{\partial\xi^2}N_e-M\frac{\partial^2}{\partial\xi^2}(N_iV_{iz}) \quad (18)$$

Integrating and solving Eqs. (15) - (18) for $\xi\to\infty,\ N\to 1, V\to 0$, we get

Here we have used Ψ<<1 and Mach number M is replaced with M_A by using the relation $V_A=\sqrt{\frac{2}{\beta'}}c_s,\ M_A=\frac{V}{V_A}=\sqrt{\frac{\beta'}{2}}\,M.$

$$K_x^2\frac{\partial^2\Psi}{\partial\xi^2}=\alpha_1\Psi+\alpha_2\Psi^2+\alpha_3\Psi^3-\frac{M_A^2}{{K_z}^2}(\alpha_1\Psi+\alpha_2\Psi^2+\alpha_3\Psi^3+\alpha_1^2\Psi^2+2\alpha_1\alpha_2\Psi^3)-\frac{\beta}{2M_A^2}(\Psi+2\alpha_1\Psi^2+\alpha_2\Psi^3+\alpha_1^2\Psi^3+\alpha_2\Psi^3)+\frac{\beta}{2}(\Psi+3\alpha_1\Psi^2+3\alpha_1^2\Psi^3+\alpha_2\Psi^3) \quad (19)$$

Integrating the above equation (19) using the Runge-Kutta-4 (RK4) method using the above-stated boundary conditions, we get the following well-known relation.

$$\frac{1}{2}\left(\frac{\partial\Psi}{\partial\xi}\right)^2+S(\Psi)=0 \quad (20)$$

Here $S(\Psi)$ is Sagdeev potential [10] and its value is given in Eq. (21). The coefficients A, B, and C depend upon α_1, α_2 and α_3 given in Eqs. (8) - (10).

$$S(\Psi)=\frac{1}{K_x^2}\left[A_1\frac{\Psi^2}{2}+A_2\frac{\Psi^3}{3}+A_3\frac{\Psi^4}{4}\right] \quad (21)$$

$$A_1=\left(\frac{\beta'}{2}\left(\frac{{K_z}^2}{M_A^2}-1\right)-\alpha_1\left(1-\frac{M_A^2}{{K_z}^2}\right)\right)$$

$$A_2=\left(\frac{3\beta'}{2}\alpha_1\left(\frac{2{K_z}^2}{3{M_A}^2}-1\right)+\alpha_1^2\frac{{M_A}^2}{{K_z}^2}-\alpha_2\left(1-\frac{{M_A}^2}{{K_z}^2}\right)\right)$$

$$A_3=\left(\frac{\beta'}{2}\left(\frac{2{K_z}^2}{M_A^2}-1\right)\alpha_2+\frac{3\beta'}{2}\alpha_1^2\left(\frac{2{K_z}^2}{3{M_A}^2}-1\right)+2\alpha_1\alpha_2\frac{{M_A}^2}{{K_z}^2}-\alpha_3\left(1-\frac{M_A^2}{{K_z}^2}\right)\right)$$

Existence Conditions for Double Layers:

A double-layer solution of Eq. (21) exists if $S(\Psi)$ satisfy the following conditions

$$S(\Psi) = 0 \text{ when } \Psi = 0, \Psi_m;$$
$$\frac{dS(\Psi)}{d\Psi} = 0 \text{ when } \Psi = 0, \Psi_m \text{ and}$$
$$\frac{d^2S(\Psi)}{d\Psi^2} < 0 \text{ when } \Psi = 0, \Psi_m$$

$$S(\Psi) = \frac{A_3}{4K_x^2}(\Psi_m - \Psi)^2\Psi^2 \qquad (22)$$

Where $\Psi_m = -\frac{2A_2}{3A_3}$. The energy integral equation takes the form.

$$\frac{1}{2}\left(\frac{\partial\Psi}{\partial\xi}\right)^2 + \frac{A_3}{4K_x^2}(\Psi_m - \Psi)^2\Psi^2 = 0 \qquad (23)$$

which have a solution

$$\Psi = \frac{\Psi_m}{2}\left[1 - tanh\sqrt{-\frac{A_3}{8K_x^2}}\Psi_m\,\xi\right] \qquad (24)$$

It shows that a real solution is possible only for $A_3 < 1$.

The relation $\Psi_m = -\frac{2A_2}{3A_3}$, shows that compressive and rarefactive double layers exist for $A_2 < 0$ and $A_2 > 0$, respectively.

The Finite Difference Method (FDM) is used to find Sagdeev potential conditions as the FDM is commonly used to solve differential equations numerically, including those governing the Sagdeev potential, which describes the nonlinear electrostatic potential of waves in plasma.

Results:

In this section, we considered Alfvenic DLs in a low-β' Electron-ion κ-distributed plasma and numerically investigated the corresponding electric field associated with these DLs using the THEMIS data (Dated: 29-02-2008 at 08: 33:48) [18]. The reported DLs have amplitude up to $\sim 25\ mV/m$, $v_s \approx 500\ km/s$, $T_e \sim 440$ keV and the corresponding potential is up to $\sim 200\ V$. In addition, the observed $E_\parallel$ Signals had a scale length of $20\ \lambda_D$, where $\lambda_D = 0.5\ km$ at the observed values of $n_e = 0.08\ \text{cm}^{-3}$ and $B = 22$ nT.

Figure 1 shows the Sagdeev potential for compressive double-layer structures for variation in κ. It is clear from the plot that the amplitude and width of the double layers increase by increasing the value of κ. Figure 2 shows the electrostatic shock structures for variation in κ. It is clear from the Figure that the shock height increases with an increase in spectral index κ. Figure 3 depicts the $E_\parallel$ For compressive double layer structures for variation in κ. It is clear from the plot that the magnitude of $E_\parallel$ Increases with the increase in spectral index κ. Figure 4 shows the Sagdeev potential for compressive double-layer structures for variation in M_A. It is clear from the plot that the amplitude and width of the double layer decreases by increasing the value of M_A. Figure 5 shows the corresponding electrostatic shock structures for variation in M_A. It is clear from the figure that the shock height decreases by increasing the value of M_A. Figure 6 shows the $E_\parallel$ for compressive double-layer structures for variation in M_A. It is clear from the Figure that. $E_\parallel$ decreases with an increase in the value of M_A.

Table 1: Comparison of numerical results with the observed values of double-layer parameters

Double Layer Parameters	$\boldsymbol{\kappa = 2}$	$\boldsymbol{\kappa = 3}$	$\boldsymbol{\kappa = 15}$	**Observed Values**
Electrostatic potential Ψ (V)	400	300	220	200

Parallel Electric field $E_{\parallel}$ (mV/m)	30	22	17	25

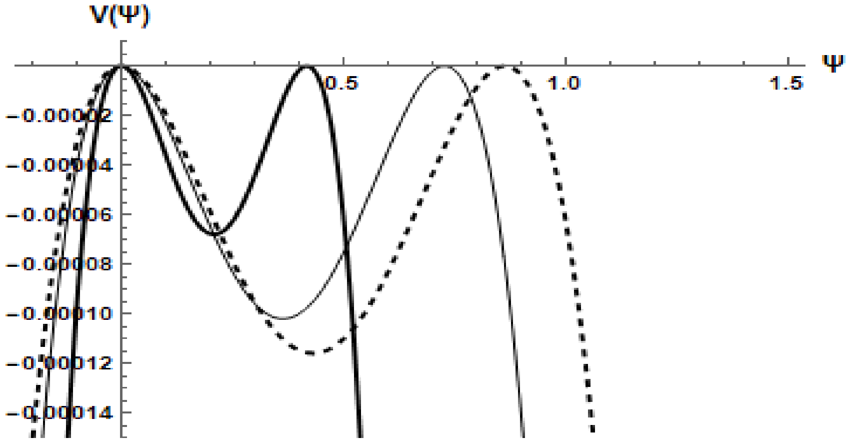

Figure 1: Compressive Sagdeev potential $\boldsymbol{V(\Psi)}$ against $\boldsymbol{\Psi}$ for $\boldsymbol{M_A = 0.18}$, $\boldsymbol{\kappa = 2}$ (Thick line), $\boldsymbol{\kappa = 3}$ (Thin Dashed line), $\boldsymbol{\kappa = 15}$ (Thick Dashed line), $\boldsymbol{\theta = 75^o}$.

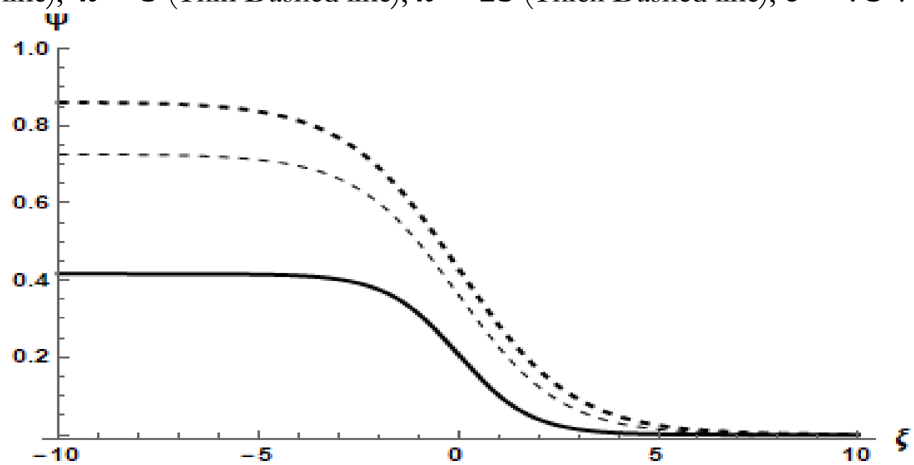

Figure 2: Compressive electrostatic potential $\boldsymbol{\Psi}$ against $\boldsymbol{\xi}$ for $\boldsymbol{M_A = 0.18}$, $\boldsymbol{\kappa = 2}$ (Thick line), $\boldsymbol{\kappa = 3}$ (Thin Dashed line), $\boldsymbol{\kappa = 15}$ (Thick Dashed line), $\boldsymbol{\theta = 75^o}$.

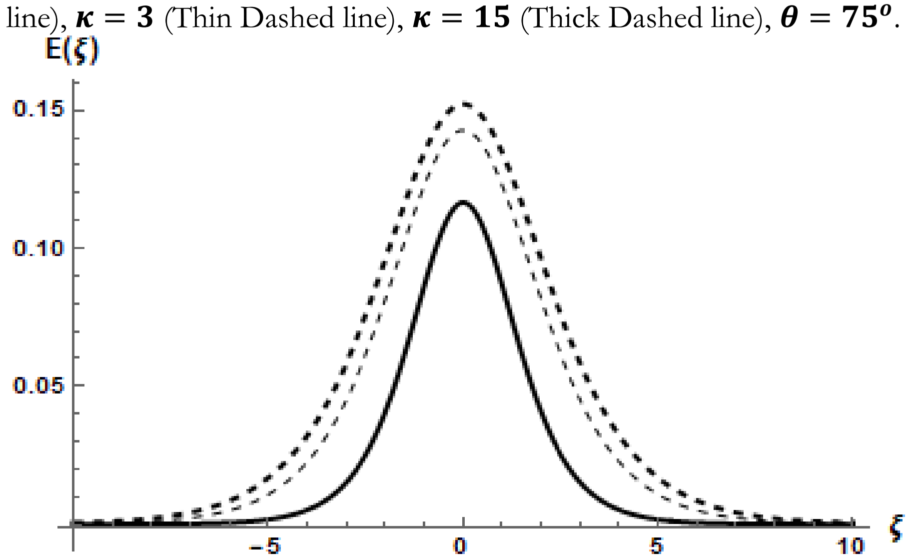

Figure 3: Parallel electric field against $\boldsymbol{\xi}$ for compressive potential structure for $\boldsymbol{M_A = 0.18}$, $\boldsymbol{\kappa = 2}$ (Thick line), $\boldsymbol{\kappa = 3}$ (Thin Dashed line), $\boldsymbol{\kappa = 15}$ (Thick Dashed line), $\boldsymbol{\theta = 75^o}$.

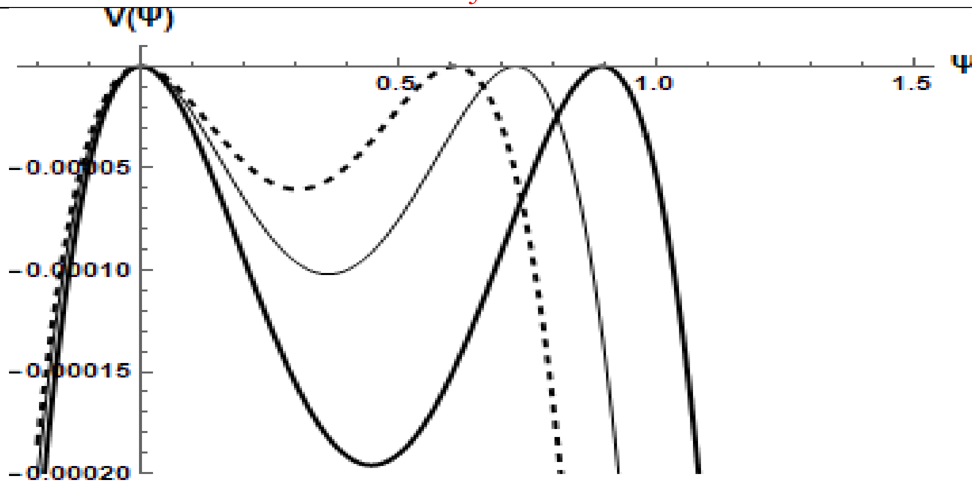

Figure 4: Compressive Sagdeev potential $\boldsymbol{V(\Psi)}$ against $\boldsymbol{\Psi}$ for, $\boldsymbol{\kappa = 2}$, $\boldsymbol{M_A = 0.17}$ (Thick line), $\boldsymbol{M_A = 0.18}$ (Thin line), $\boldsymbol{M_A = 0.19}$ (Dashed line), $\boldsymbol{\theta = 75^o}$.

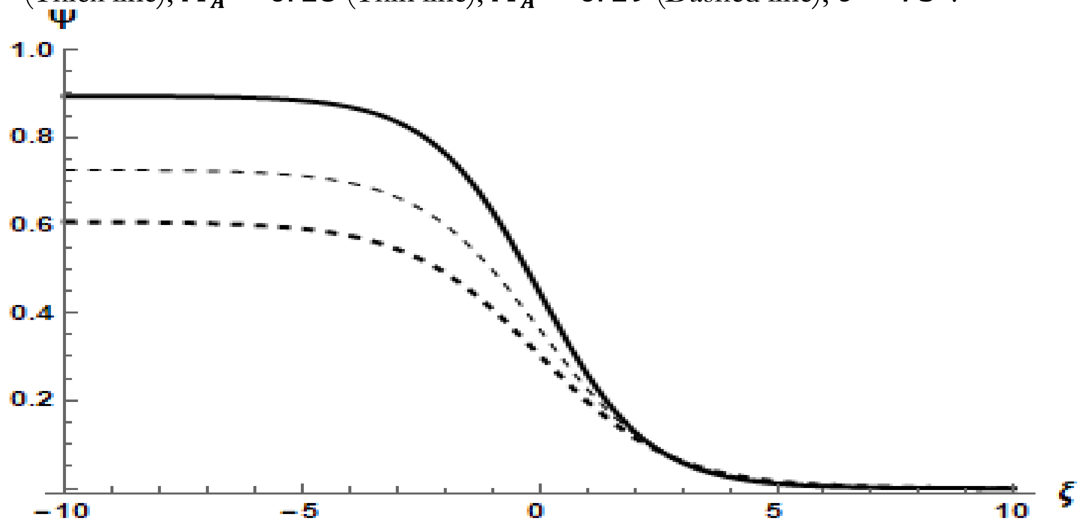

Figure 5: Compressive electrostatic potential $\boldsymbol{\Psi}$ against $\boldsymbol{\xi}$ for $\boldsymbol{\kappa = 2}$, $\boldsymbol{M_A = 0.17}$ (Thick line), $\boldsymbol{M_A = 0.18}$ (Thin line), $\boldsymbol{M_A = 0.19}$ (Dashed line), $\boldsymbol{\theta = 75^o}$.

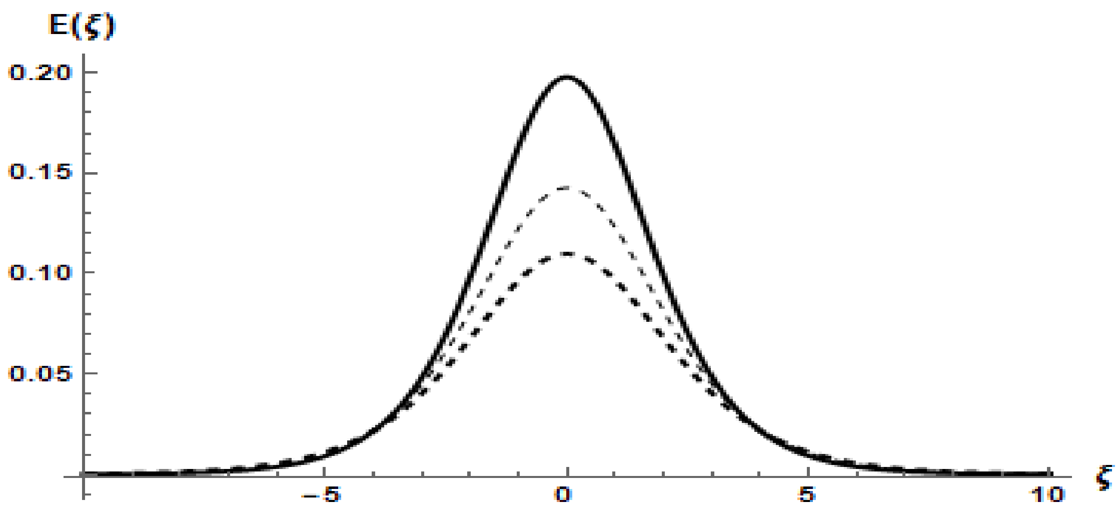

Figure 6: Parallel electric field against $\boldsymbol{\xi}$ for compressive potential cure for, $\boldsymbol{\kappa = 2}$, $\boldsymbol{M_A = 0.17}$ (Thick line), $\boldsymbol{M_A = 0.18}$ (Thin line), $\boldsymbol{M_A = 0.19}$ (Dashed line), $\boldsymbol{\theta = 75^o}$.

Discussion:

Our Results showed that compressive Alfvenic double layers (DLs) exist in kappa-distributed electron-ion plasma. We analyzed the dependence of the double-layer structure on Alfvenic Mach number. M_A And spectral index κ. The Sagdeev potential analysis suggested that increasing κ, increases the width and amplitude of the double-layer structure. Electrostatic shock structure also showed an increase in shock height by increasing κ. Moreover, the parallel electric field increases with increasing κ, showing a strong dependence of these parallel potential structures upon non-Maxwellian spectral index κ. Analyzing the effect of M_A on these double-layer structures showed that increasing the value of M_A, the amplitude and width of the double layer decrease. This indicates a reduction in the strength of double layers. Also, the shock heightened and the associated electrostatic field decreased with an increase in M_A.

The present study investigates the dynamics of coupled kinetic Alfven-acoustic (CKAA) waves in a collisionless, magnetized electron-ion plasma with non-Maxwellian electrons described by a kappa distribution. The analysis is conducted within the framework of both linear and nonlinear theories, incorporating a low-β plasma approximation. Our model builds on the two-potential formalism in which the electrostatic potentials ψ and ϕ represent the parallel and perpendicular components of the electric field with respect to the ambient magnetic field, respectively.

The utilization of a kappa-distributed electron population reflects a more realistic scenario in space and astrophysical plasmas where suprathermal electrons are commonly observed. These high-energy tails significantly alter the pressure dynamics and hence the overall wave characteristics. The expressions for electron number density [Eq. (7)] and modified temperature [Eq. (13)] emphasize the impact of the spectral index ϰ on the local thermodynamic behavior of electrons. As ϰ decreases (but remains >3/2), the deviation from Maxwellian behavior becomes more prominent, increasing the effective temperature and hence modifying the dispersion and nonlinear structures of CKAA waves.

The coupling between electrostatic and electromagnetic wave modes in our model gives rise to hybrid CKAA modes that blend properties of both kinetic Alfven waves (KAWs) and ion acoustic waves. These waves are of particular relevance in environments like the solar wind, Earth's magnetosphere, and laboratory plasmas, where low-frequency electromagnetic perturbations coexist with density inhomogeneities and nonthermal particle distributions.

The derived linear dispersion relation [Eq. (14)] captures the essential interplay between the ion-sound speed csc_scs, the Alfven speed VAV_AVA, and the influence of nonthermal electrons through the coefficient α1\alpha_1α1. A key insight from this relation is that the CKAA wave frequency is enhanced in the presence of strong electron nonthermal populations (i.e., lower ϰ values). This enhancement arises from the elevated pressure and temperature of the ϰ-distributed electrons, which in turn raise the effective ion-sound speed csc_scs. The condition ω2≪Ωi2ω^2 ≪ Ω_i^2ω2≪Ωi2, valid for low-frequency perturbations, ensures that higher-order gyrokinetic effects are suppressed, simplifying the analytic treatment.

In the long-wavelength limit, the dispersion relation simplifies to a form akin to that of kinetic Alfven waves, yet modified by λsλ_sλs, a term incorporating the transverse wave vector kxk_xkx and the ion gyroradius ϱsϱ_sϱs. This reduction illustrates the smooth transition between purely electrostatic ion acoustic waves and electromagnetic Alfvenic modes within the same theoretical framework, contingent on wave parameters and plasma conditions.

The nonlinear treatment using Sagdeev potential formalism yields a comprehensive understanding of large-amplitude solitary and double layer structures in CKAA waves. The normalization of governing equations and transformation into the co-moving frame reveal the conserved quantities and allow for an effective exploration of nonlinear stationary states. The emergence of double layer solutions suggests the potential for localized, nonlinear electric field structures which may transport energy and particles over macroscopic distances.

Physically, these double layers can form due to imbalance in ion and electron pressure gradients induced by nonthermal electrons. The results support the notion that in strongly magnetized plasmas, such nonlinear structures can persist and may play an essential role in plasma transport and turbulence.

The dependence of the Sagdeev potential on ϰϰϰ, Mach number MMM, and obliqueness parameters Kx,KzK_x, K_zKx,Kz indicates that the existence and nature of solitary and double layer solutions are sensitive to both plasma composition and geometry. Specifically, lower values of ϰ (i.e., higher nonthermality) tend to broaden the width of solitary waves and increase their amplitude, as greater electron pressure supports stronger electrostatic potential gradients.

This study extends previous models by incorporating kappa distributions in both linear and nonlinear analyses of CKAA waves, whereas earlier works often assumed Maxwellian equilibrium (i.e., ϰ→∞). For instance, comparisons with models by Saleem (1999) and Hafez et al. (2021) reveal that kappa-distributed systems allow for richer nonlinear phenomena and more pronounced dispersion modifications. Moreover, the impact of two-potential theory, as emphasized in this work, adds another layer of realism, allowing for anisotropic field structures that are often ignored in simpler one-potential models.

Furthermore, the presence of double layers and steep potential gradients aligns with observations from spacecraft missions such as THEMIS and Cluster, where abrupt changes in electric potential and density have been detected in magnetospheric boundary layers and plasma sheets. From a broader perspective, the findings of this study are relevant to understanding energy dissipation, wave-particle interactions, and anomalous transport in space plasmas. The ability of CKAA waves to support double layers may also have implications for auroral acceleration mechanisms and plasma heating in the solar corona.

In future work, this model can be extended to include additional complexities such as finite ion temperature effects, multi-ion species, or relativistic corrections. Another promising avenue is the inclusion of dissipative effects such as Landau damping or collisions, which may affect the stability and longevity of nonlinear structures. A comparison between simulation data and analytical Sagdeev potentials may also help in validating the theoretical predictions presented here.

These results highlighted how double-layer characteristics depend upon the non-Maxwellian distribution function and M_A. Our findings highlighted the importance of non-Maxwellian distributed plasmas as compared to Maxwellian distributed plasmas.
We have shown the exact values of shock potential and electric field in Table. 1. It shows that these values are in good agreement with the observed values.

Conclusion:

In this paper, we have investigated the parallel electric field structures associated with Alfvenic double layers in low beta electron-ion plasmas. We have considered electrons to be κ-distributed and calculated the plasma beta for those values of plasma parameters that are observed by THEMIS in PSBL of Earth's magnetosphere. These kinds of structures are also seen naturally in magnetic field reconnection sites and the solar wind as well. It is a universal phenomenon to observe parallel electric fields linked to DLs in collisionless plasmas and numerous active plasma areas as stated above. Our theoretical and numerical investigations support the existence of compressive double layers and positive potential structures. We found that the amplitude of shock structures and electric fields increases with the increase in spectral index κ but decreases with the increase in Mach number. The numerical results of the potential and electric fields successfully interpret the observed values of electric field and potential structures in PSBL in particular and other space plasma regions in general.

References:

[1] M. André, A. Vaivads, S. C. Buchert, A. N. Fazakerley, "Thin electron-scale layers at the magnetopause," *Geophys. Res. Lett.*, 2004, doi: https://doi.org/10.1029/2003GL018137.

[2] J. F. Drake, M. A. Shay, W. Thongthai, and M. Swisdak, "Production of energetic electrons during magnetic reconnection," *Phys. Rev. Lett.*, vol. 94, no. 9, p. 095001, Mar. 2005, doi: 10.1103/PHYSREVLETT.94.095001.

[3] P. L. Pritchett, F. V. Coroniti, "Three-dimensional collisionless magnetic reconnection in the presence of a guide field," *J. Geophys. Res. Sp. Phys.*, 2004, doi: https://doi.org/10.1029/2003JA009999.

[4] A. Vaivads, A. Retinò, and M. André, "Magnetic reconnection in space plasma," *Plasma Phys. Control. Fusion*, vol. 51, no. 12, p. 124016, Nov. 2009, doi: 10.1088/0741-3335/51/12/124016.

[5] I. Y. Vasko, R. Wang, F. S. Mozer, Stuart D. Bale, *et al.*, "On the Nature and Origin of Bipolar Electrostatic Structures in the Earth's Bow Shock," *Front. Phys*, vol. 8, 2020, doi: https://doi.org/10.3389/fphy.2020.00156.

[6] M. A. Raadu, "Particle acceleration mechanisms in space plasmas," *Phys. Chem. Earth, Part C Solar, Terr. Planet. Sci.*, vol. 26, no. 1–3, pp. 55–59, 2001, doi: https://doi.org/10.1016/S1464-1917(00)00090-8.

[7] F. S. Mozer, C. A. Kletzing, "Direct observation of large, quasi-static, parallel electric fields in the auroral acceleration region," *Geophys. Res. Lett.*, 1998, doi: https://doi.org/10.1029/98GL00849.

[8] L. Fletcher and H. S. Hudson, "Impulsive Phase Flare Energy Transport by Large-Scale Alfvén Waves and the Electron Acceleration Problem," *Astrophys. J.*, vol. 675, no. 2, 2008, doi: https://doi.org/ 10.1086/527044.

[9] D. J. Gershman, Adolfo F Vinas, John C. Dorelli, S. A. Boardsen, *et al.*, "Wave-particle energy exchange directly observed in a kinetic Alfvén-branch wave," *Nat. Commun.*, vol. 8, no. 1, p. 14719, 2017, doi: https://doi.org/10.1038/ncomms14719.

[10] Saba Khalid, M. N. S. Qureshi, and W. Masood, "Compressive and rarefactive solitary structures of coupled kinetic Alfven-acoustic waves in non-Maxwellian space plasmas," *Phys. Plasmas*, vol. 26, no. 9, Sep. 2019, doi:https://doi.org/10.1063/1.5115478/263564.

[11] H. A. Shah, W. Masood, M. N. S. Qureshi, P. H. Yoon, "Nonlinear kinetic Alfvén waves with non-Maxwellian electron population in space plasmas," *J. Geophys. Res. Sp. Phys.*, 2015, doi: https://doi.org/10.1002/2014JA020459.

[12] V. M. Vasyliunas, "A survey of low-energy electrons in the evening sector of the magnetosphere with OGO 1 and OGO 3," *J. Geophys. Res.*, vol. 73, no. 9, pp. 2839–2884, May 1968, doi: https://doi.org/10.1029/JA073I009P02839.

[13] N. F. Cramer, "The physics of Alfvén waves," *John Wiley Sons*, 2001, [Online]. Available: https://download.e-bookshelf.de/download/0000/6039/10/L-G-0000603910-0002364724.pdf

[14] A. F. Viñas, Pablo S. Moya, Roberto E. Navarro, J. A. Valdivia, *et al.*, "Electromagnetic fluctuations of the whistler-cyclotron and firehose instabilities in a Maxwellian and Tsallis-kappa-like plasma," *J. Geophys. Res. Sp. Phys.*, 2015, doi: https://doi.org/10.1002/2014JA020554.

[15] V. Pierrard and M. Lazar, "Kappa Distributions: Theory and Applications in Space Plasmas," *Sol. Phys.*, vol. 267, no. 1, pp. 153–174, Nov. 2010, doi: https://doi.org/10.1007/S11207-010-9640-2.

[16] E. M. Lifshitz and L. P. Pitaevskii, "Physical Kinetics"-Evgeniĭ Mikhaĭlovich Lifshit͡s, Lev Petrovich Pitaevskiĭ - Google Books," Pergamon Press. Accessed: Mar. 09, 2025. [Online]. Available: https://books.google.com.pk/books/about/Physical_Kinetics.html?id=tQNTIOPaJukC&redir_esc=y.
[17] Saba Khalid, M. N. S. Qureshi, and W. Masood, "Nonlinear kinetic Alfven waves in space plasmas with generalized (r, q) distribution," *Astrophys. Space Sci.*, vol. 363, no. 10, pp. 1–9, Oct. 2018, doi: https://doi.org/10.1007/S10509-018-3444-5/METRICS.
[18] R. E. Ergun, L. Andersson, J. Tao, V. Angelopoulos, *et al.*, "Observations of double layers in earth's plasma sheet," *Phys. Rev. Lett.*, vol. 102, no. 15, Apr. 2009, doi: https://doi.org/10.1103/PHYSREVLETT.102.155002.